A study of randomness, correlations, and collectivity in the nuclear shell model

V. Velázquez, J. G. Hirsch, and A. Frank
Instituto de Ciencias Nucleares, Universidad Nacional Autónoma de México, Apartado Postal 70-543, 04510 México, Distrito Federal, Mexico

A. P. Zuker
IRES, bât 27, IN2P3-CNRS Université Louis Pasteur, Boîte Postale 28, F-67037 Strasbourg, Cedex 2, France
(Received 27 August 2002; published 24 March 2003)

A variable combination of realistic and random two-body interactions allows the study of collective properties [such as the energy spectra and $B(E2)$ transition strengths] in ^{44}Ti, ^{48}Cr, and ^{24}Mg. It is found that the average energies of the yrast band states maintain the ordering for any degree of randomness, but the $B(E2)$ values lose their quadrupole collectivity when randomness dominates the Hamiltonian. The high probability of the yrast band to be ordered in the presence of pure random forces exhibits the strong correlations between the different members of the band.

DOI: 10.1103/PhysRevC.67.034311 PACS number(s): 21.10.Re, 05.30.Fk, 21.60.Cs, 23.20.−g

I. INTRODUCTION

Nuclei display very regular spectral patterns. Low energy states in medium- and heavy-mass even-even nuclei allow their classification in terms of seniority, anharmonic vibrator, and rotor nuclei [1], according to the ratio of the excitation energies of the states 4_1 and 2_1. While this regular behavior has been usually related with specific forces, the investigation of the energy spectra with random interactions [2,3] has shown that many-body states are strongly correlated even in the presence of random two-body interactions. Random interactions in bosonic Hilbert spaces, like those used in the IBM and the vibron model, exhibit a large predominance of vibrational and rotational spectra, strongly suggesting that in boson spaces collectivity is an intrinsic property of the space of nuclear states [4–6]. Recently, several studies were performed with random and displaced random ensembles in order to simulate realistic systems [7,8], in particular, to investigate the dominance of $0+$ states [9,10].

In the nuclear shell model the transition between random and collective behavior in the energy spectra of ^{20}Ne generated by two-body forces was addressed in Ref. [11]. Collectivity was generated with a quadrupole-quadrupole force, while a residual random interaction was included in the Hamiltonian in order to study its consequences on the system's spectroscopic properties. Both the eigenvalue distribution and the overlap between the SU(3) and calculated wave functions exhibit the smooth path from a Hamiltonian dominated by the collective force to a random, noncollective one.

The present work aims to extend these ideas by studying the transition from a realistic parametrization of the two-body force to a purely random one, in complex systems such as ^{24}Mg, ^{44}Ti, and ^{48}Cr. The realistic interactions we have chosen are the universal Wildenthal [12] interaction for the sd shell, and the Kuo and Brown (KB3) interaction [13] for the fp shell. The probability for each state in the yrast band to follow a sequence where the higher energies correspond to the states with the larger angular momentum is studied by varying the mixing between realistic and random forces in the Hamiltonian. The evolution of the average energies for each member of the band, as well as its $B(E2)$ values, is also reported.

II. BAND STRUCTURE

The combination of random and realistic interactions is taken [11] as

$$H = aH_C + bH_R, \quad \text{with} \quad a+b=1, \tag{1}$$

where H_C is a realistic Hamiltonian and H_R is a two-body random ensemble. Both H_C and H_R are written [14] as

$$H = \sum_{r\leq s,t\leq u} V^{JT}_{rstu} Z^{\dagger}_{rs,JT} Z_{tu,JT} \tag{2}$$

in terms of scalar products of the normalized pair creation operators $Z^{\dagger}_{ij,JT}$ and its Hermitian conjugate $Z_{kl,JT}$, where r,s, etc. specify subshells associated with individual orbits, and J,T are the coupled angular momentum and isospin. For the realistic Hamiltonian, V^{JT}_{rstu} is the Wildenthal or KB3 interaction. For the random case the V^{JT}_{rstu} matrix elements are taken from a two-body random ensemble, i.e., to be real and normally distributed with mean zero and width σ for the off-diagonals and $\sqrt{2}\sigma$ for the diagonals. The values of the width σ are taken from the realistic interactions: 1.34 MeV and 0.60 MeV, for the sd and fp shells, respectively. The parameter b is varied from 0 to 1, to cover the different mixing from the realistic interaction to a pure random force.

Calculations are performed in the full valence space for both ^{44}Ti and ^{24}Mg. For ^{48}Cr we use the truncated $f_{7/2}p_{3/2}$ subspace, which allows for repetitive shell-model calculations in affordable times, and at the same time contains most of the relevant degrees of freedom, as a consequence of the ''quasi-SU(3) symmetry'' [19]. In this basis the energy spectra is definitively rotational [8].

For the three nuclei, the absence of a single-particle term makes Hamiltonian (2) more collective than in usual shell-model calculations. In the three examples discussed below, the energy spectra obtained for $b=0$ exhibit little effect due to the lack of single-particle energies, while the $B(E2)$ tran-

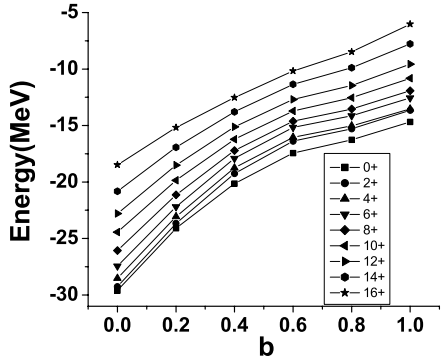

FIG. 1. Average energy of 960 runs for each angular momentum of the ground-state band in ^{48}Cr.

sition strengths are enhanced by 50%, except in the case of ^{48}Cr, where the use of a truncated space limits the $B(E2)$ value.

A. The *fp* shell

As a first example we take ^{48}Cr, a rotational nucleus that has been widely studied in full shell-model calculations. In the present case the diagonalization is performed in the $f_{7/2}p_{3/2}$ shell with the code ANTOINE [15], using a KB3 interaction [13] without single-particle energies.

Figure 1 shows the average energies E_J of the lowest energy state for each angular momentum $J=0\hbar, 2\hbar, \ldots, 16\hbar$, the yrast band, calculated for 960 samples of the random interaction.

The vertical axis displays the average energy of each state, as a function of the mixing parameter b. At the left hand side the realistic shell-model energies are shown, with its distinctive rotor pattern, which resembles closely the exact yrast band. As b increases to the right, the order between the different members of the bands is maintained, but their relative separation changes. The average energies in the right hand side, the pure random Hamiltonian, still exhibit a band structure but have lost their quadrupole collectivity, as discussed below in connection with their $B(E2)$ values.

The evolution of the average ground-state (gs) band of ^{44}Ti, calculated in the full pf shell, is shown in Fig. 2 as a

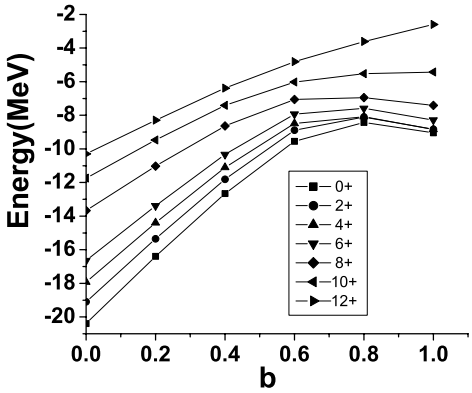

FIG. 2. Average energy of 960 runs for each angular momentum of the ground-state band in ^{44}Ti.

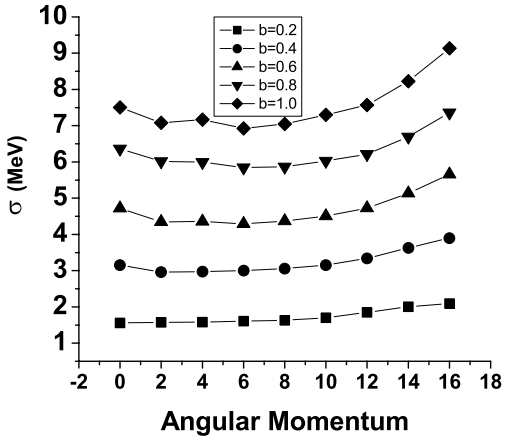

FIG. 3. Average energy width of 960 runs for each angular momentum of the ground-state band in ^{48}Cr.

function of the mixing parameter b. It can be seen that the relative ordering of the states with different angular momentum is maintained, but their relative separations vary significantly in the transition from the realistic to the random Hamiltonian. However, up to $b=0.6$ the change is mostly a scale variation, with the nearly equidistant structure of the band keeping its form. The energy spectra evolve from a vibrational equidistant form at $b=0$ to a mixed, yet ordered, spectrum for pure random forces. The average ground-state energy increases with the increase in mixing to a maximum value, with a slight decrease for $b=1$.

Similar patterns of evolution of the energy centroids for each angular momentum, as a function of the mixing parameter, were found in several other nuclei such as ^{46,48}Ca and ^{46}Ti. While for ^{46}Ti, the centroid of the $J=2$ state is lower in energy than the $J=0$ state for a pure random Hamiltonian, in general, for these nuclei and others in the sd shell the average energy ordering is conserved, and there is a gradual change in the energy spectra.

The width σ associated with the lowest average energy for each angular momentum, calculated as the square root of the variance, is shown in Fig. 3 for the gs band of ^{48}Cr, as a function of the angular momentum, for different values of

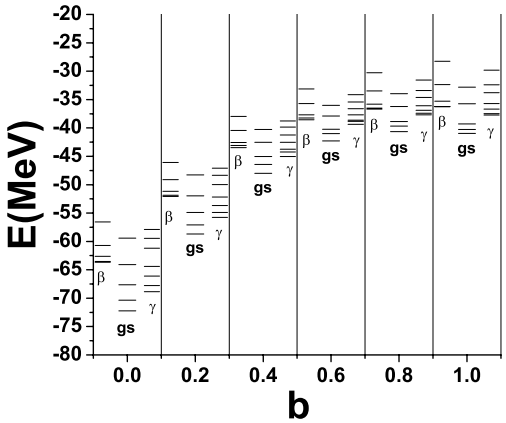

FIG. 4. Average energy of 960 runs for each angular momentum of three bands in ^{24}Mg; see text for label description.

TABLE I. Probability for each angular momentum state to be in the correct position in the ground-state band with $b=0.4$ for ^{48}Cr.

$J+$	1st	2nd	3rd	4th	5th	6th	7th	8th	9th
0	96.56	1.04	1.25	0.52	0.42	0.10	0.00	0.10	0.00
2	1.56	91.88	5.31	0.62	0.21	0.21	0.10	0.00	0.10
4	0.21	5.62	92.29	1.04	0.42	0.21	0.21	0.00	0.00
6	0.52	0.94	0.42	92.50	4.27	0.94	0.21	0.00	0.21
8	0.73	0.21	0.21	3.75	93.02	1.04	0.31	0.52	0.21
10	0.00	0.00	0.10	0.83	0.52	95.21	2.29	0.83	0.21
12	0.00	0.00	0.21	0.62	0.83	2.08	96.04	0.21	0.00
14	0.21	0.21	0.10	0.10	0.31	0.10	0.52	97.40	1.04
16	0.21	0.10	0.10	0.00	0.00	0.10	0.31	0.94	98.23

the mixing parameter b. The energy width increases with the increase in mixing, from 1.5 MeV for $b=0.2$ to 7–9 MeV for $b=1.0$. Given that, as b increases, these widths become larger than the gaps between the average energies, they indicate a strong mixing between different bands, an effect closely associated with the lack of collectivity discussed below. As a function of the angular momentum all the widths are essentially flat, showing a moderate increase for the largest angular momenta.

The energy widths are larger than the relative energy differences between adjacent states in the gs band, implying that there are individual cases in which the spectrum is not ordered. However, the number of runs with a completely ordered spectrum is large even for pure random interactions, as is discussed in detail below.

B. The *sd* shell

Calculations in the sd shell can be done for the full shell and an arbitrary number of active particles. The realistic interaction used in this case is the universal Wildenthal interaction [12]. The nucleus ^{24}Mg offers a rich enough system, where three bands can be studied simultaneously. They correspond, for $b=0$, to the gs, β, and γ bands. The first two start with $J=0$ and contain only even-J states, while the γ band starts with $J=2$ and includes states with both even and odd angular momenta, up to $J=8$. Following the evolution of the average energy levels as the mixing parameter b increases, we reconstruct the three bands for each value of b. Nevertheless, for a pure random interaction one can show that the states have lost their quadrupole collectivity (see below), and for this reason they do not form bands in the usual sense.

In Fig. 4 the average energies for each angular momentum, for the ground state, β, and γ bands in ^{24}Mg, are presented for different values of the mixing parameter b.

The most relevant features observed in Fig. 4 are that the three bands evolve in a similar way, keeping their internal order as well as the relative separation between the bands. The correlation between increasing energy and angular momentum is strictly followed in all the averaged bands. The absolute ground-state energy becomes larger as the mixing parameter increases, following the same pattern found in the fp shell.

III. ORDERING PROBABILITIES

In order to further study these systems, we have analyzed the probability that each state in the band has the usual ordering; i.e., the largest the angular momentum, the highest the energy for a given band. To do so, we counted the number of runs where the first $J=0$ state is the ground state, the

TABLE II. Probability for each angular momentum state to be in different positions, for the ^{48}Cr ground-state band with $b=1.0$.

$J+$	1st	2nd	3rd	4th	5th	6th	7th	8th	9th
0	60.31	8.85	9.27	4.48	4.90	2.50	1.98	2.29	5.42
2	17.40	43.54	16.98	4.17	3.96	2.60	3.12	5.00	3.23
4	6.56	27.71	47.08	6.46	2.40	2.71	4.38	2.19	0.52
6	2.40	5.42	9.79	64.58	6.25	5.31	3.12	1.77	1.35
8	3.12	3.65	4.69	9.06	69.58	6.46	1.15	1.56	0.73
10	1.35	2.50	3.44	5.94	7.19	74.69	3.54	0.62	0.73
12	1.98	1.88	5.52	2.50	3.23	3.65	79.06	1.98	0.21
14	1.15	5.62	1.98	1.67	0.94	1.25	2.40	80.10	4.90
16	5.73	0.83	1.25	1.15	1.56	0.83	1.25	4.48	82.92

TABLE III. Probability for each angular momentum to be in different positions, for the ^{44}Ti ground-state band, with $b=1.0$.

$J+$	1st	2nd	3rd	4th	5th	6th	7th
0	46.25	19.27	20.42	6.98	5.62	1.35	0.10
2	16.56	39.90	24.38	11.56	5.83	1.25	0.52
4	21.04	25.83	40.10	9.38	3.02	0.21	0.42
6	8.44	10.42	10.10	64.58	5.42	1.04	0.00
8	6.56	3.96	4.27	5.83	76.77	2.08	0.52
10	0.10	0.52	0.52	1.25	2.60	92.08	2.92
12	1.04	0.10	0.21	0.42	0.73	1.98	95.52

first excited state in the band, the second excited state, and so on, in the 960 runs. We did the same for the states with angular momenta $J=2$, 4, etc. In Table I the percentages for ^{48}Cr with a mixing of $b=0.4$ are listed. All the states have a probability of at least 90% to occupy its physically expected place, while the dispersion is very small.

Table II lists the probability for states of each angular momentum in ^{48}Cr to occupy the indicated place for a purely random Hamiltonian, i.e., $b=1$. The probabilities of being in its expected place run from 44% for $J=2$ to 83% for $J=16$. States with $J=0$, 2, and 4 are those which more often fail to occupy their place, as they tend to exchange positions. These results represent an extension of previous studies concerning the probability of each state to be the ground state, listed in the first column [16].

Table III displays the probability for each angular momentum state to be in a given position, in the ^{44}Ti ground-state band with $b=1.0$. These probabilities have values ranging from 44% for $J=2$ to 95% for $J=12$. The fact that the states with $J=2$ and 4 have less than 50% probability of occupying in their places is strongly connected with the closeness of their average energies, shown in Fig. 2 for $b=1$.

Tables IV–VI display the probability that states with different angular momenta in ^{24}Mg have to occupy a given place in each band for $b=1.0$, for the ground-state, β, and γ bands, respectively. In most cases the diagonal probability, i.e., the probability that each state occupies its expected place, is larger than 50%. The exceptions are the states with $J=2$ and 3 in the γ band, and those with $J=0$ and 2 in the β band, whose probabilities lie between 38% and 48%.

TABLE IV. Probability for states belonging to the ground-state band in ^{24}Mg, with $b=1.0$, to occupy different positions.

$J+$	1st	2nd	3rd	4th	5th
0	56.56	12.40	12.29	6.77	11.98
2	18.12	52.81	13.12	9.79	6.15
4	9.06	19.58	63.85	5.52	1.98
6	4.38	11.25	6.98	71.25	6.15
8	11.88	3.96	3.75	6.67	73.75

TABLE V. The same as in Table IV, for the γ band.

$J+$	1st	2nd	3rd	4th	5th	6th	7th
2	45.21	22.92	7.50	5.94	4.79	6.46	7.19
3	27.40	38.33	13.54	6.15	4.17	6.04	4.38
4	7.40	14.90	50.62	15.94	7.29	3.02	0.83
5	7.71	12.08	15.10	58.85	5.00	1.04	0.21
6	3.44	3.75	6.25	7.60	66.25	11.88	0.83
7	5.10	4.27	4.17	3.96	10.83	64.38	7.29
8	3.75	3.75	2.81	1.56	1.67	7.19	79.27

IV. COLLECTIVITY

A sensitive measure of the quadrupole collectivity of the system is the $B(E2,2_1\rightarrow 0_{gs})$ transition strength. The distribution of $B(E2)$ strengths in ^{48}Cr, for four different values of the mixing parameter b, is shown in Fig. 5.

Its experimental value is 321 e^2 fm^2. In the restricted Hilbert space including only the $f_{7/2}p_{3/2}$ subshells, even in the absence of single-particle energies in Hamiltonian (2), this value is underestimated.

For $b=0.2$, shown in Fig. 5(a), the distribution is concentrated around 230 e^2 fm^2. For $b=0.4$, Fig. 5(b), the increase in the random components of the Hamiltonian leads to an important fragmentation of the $B(E2)$ intensity with four clusters. Among them one is near zero, the second one around 75 e^2 fm^2, the next one near 170 e^2 fm^2, and the last one close to the measured value. For $b=0.6$, Fig. 5(c), most of the $B(E2)$ values are very small, with some intensity at the collective $B(E2)$ values. Finally, in Fig. 5(d) the distribution of $B(E2)$ values for a purely random Hamiltonian is shown. It is strongly concentrated at very small values, showing a complete lack of quadrupole collectivity, in consonance with the findings of Ref. [11].

Figure 6 displays the distribution of $B(E2,2\rightarrow 0)$ values for ^{44}Ti. Figure 6(a) shows the results for $b=0.2$, with a narrow distribution around the 140 e^2 fm^2, overestimating the transition strength, which has a measured value of 120 e^2 fm^2. In Fig. 6(b) the distribution for $b=0.4$ is presented, which is concentrated around the same value. For $b=0.6$, Fig. 5(c), the distribution is still concentrated around the collective $B(E2)$ values despite the dominance of the random component in the Hamiltonian. However, this collectivity is completely lost when pure random forces are employed, as shown in Fig. 5(d).

A useful indicator of collectivity is the energy ratio

TABLE VI. The same as in Table IV, for the β band.

$J+$	1st	2nd	3rd	4th	5th
0	46.67	20.73	13.54	8.44	10.62
2	28.02	47.40	12.81	8.44	3.33
4	13.23	19.27	65.62	1.88	0.00
6	6.35	9.38	5.94	77.50	0.00
8	5.73	3.23	2.08	3.75	85.21

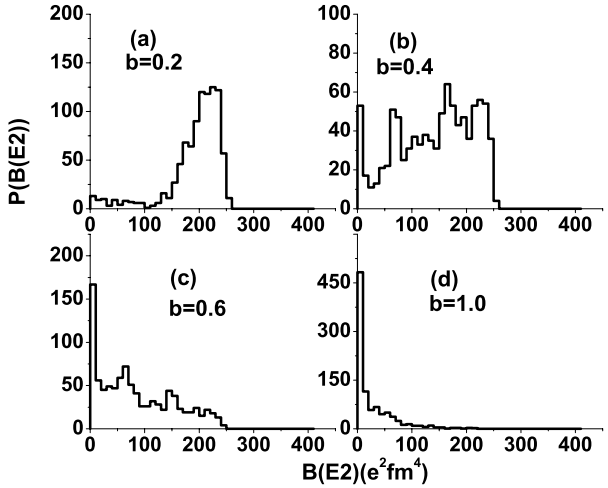

FIG. 5. Probability densities for $B(E2,2\rightarrow 0)$ for ^{48}Cr.

$$R=\frac{E_{4_1^+}}{E_{2_1^+}}. \tag{3}$$

The value $R=2$ is associated with a harmonic oscillator spectrum, while $R=3.3$ characterizes a rigid rotor structure.

Figure 7 shows the distribution of energy ratios for ^{48}Cr. The case $b=0.2$, shown in Fig. 7(a), does exhibit the actual rotor behavior of this nucleus. This feature remains dominant for $b=0.4$, Fig. 7(b), while for $b=0.6$ the distribution of energy ratios is wide and peaked at $R=1$. For $b=1.0$, shown in Fig. 7(d), the distribution is very wide, with a clear dominance of the $R=1$ ratio, in correspondence with the near degeneracy of the states with $J=2$ and 4 for $b=1$, as shown in Fig. 1.

^{44}Ti has a structure closer to a harmonic oscillator than to a rotor. This feature can be seen in Fig. 8(a), which displays the distribution of energy ratios for $b=0.2$, narrowly concentrated around $R=2$. For $b=0.4$ and 0.6, Figs. 8(b) and 8(c), the vibrational structure is wider but well defined. For a pure random interaction, Fig. 8(d), the distribution is peaked

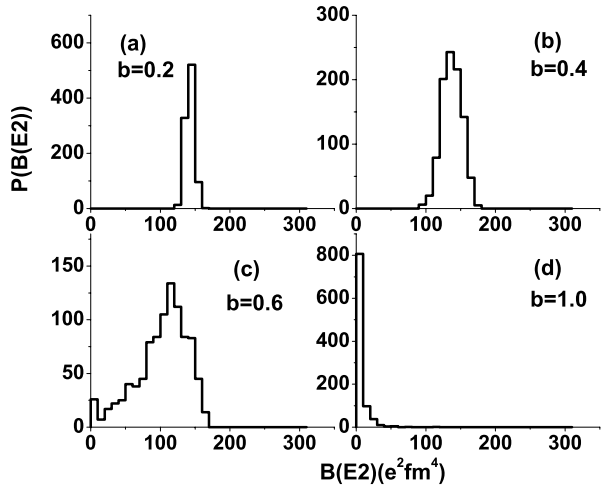

FIG. 6. Probability density for $B(E2,2\rightarrow 0)$ for ^{44}Ti.

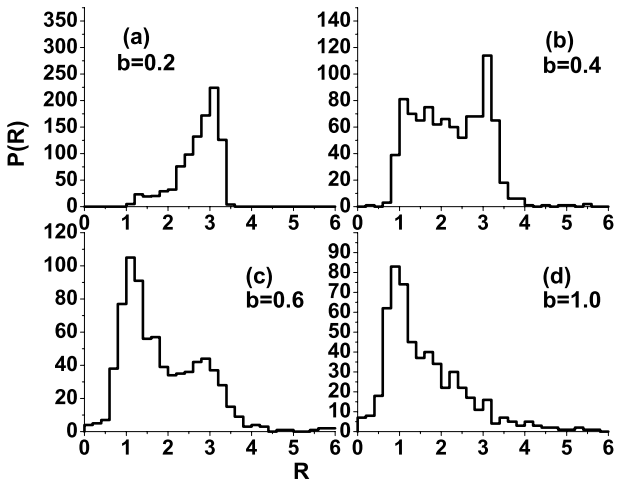

FIG. 7. Probability densities for the energy ratios R for ^{48}Cr.

at $R=1$, reflecting the near degeneracy of the average energies $\overline{E_2}$ and $\overline{E_4}$. The displacement of the most probable energy ratio R to 1 is accompanied by a lack of quadrupole coherence, consistent with the previous analysis of the $B(E2)$ transition strengths.

V. CORRELATION AND COHERENCE

Having discussed the evolution of the energy centroids as a function of the mixing parameter b, and the probability for each state to occupy a certain position in the band, it is natural to study the probability that the ground-state band has all its states properly ordered. This probability, given as the percentage of results from the 960 runs which are properly ordered, is shown in Fig. 9 for ^{48}Cr, ^{44}Ti, and ^{24}Mg. In the three cases it is apparent that the spectrum is always ordered when the realistic interaction dominates the Hamiltonian, and that the probability for the ground-state band to be ordered decreases to about 35% for a fully random Hamiltonian.

It is worth emphasizing that if these probabilities were independent of each other, the probability of finding a com-

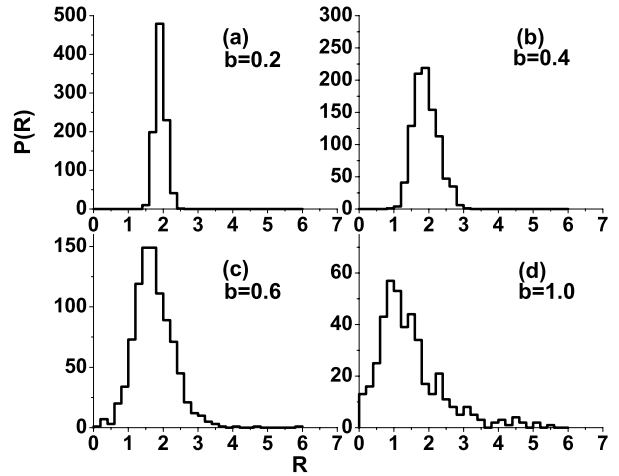

FIG. 8. Probability densities for energy ratios R for ^{44}Ti.

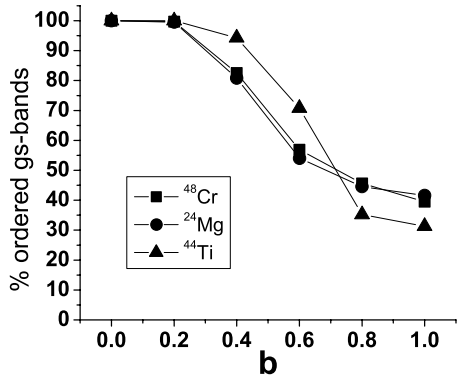

FIG. 9. Percentage of ordered bands vs *b* for Cr, Ti, and Mg.

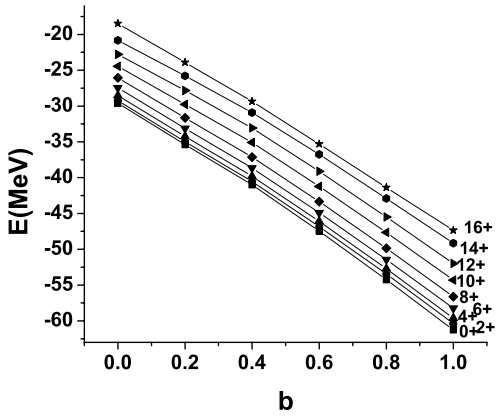

FIG. 10. Average energy of 960 runs for each angular momentum of the ground-state band in ^{48}Cr with a DTBRE mixing.

pletely ordered band would be the product of the probabilities for each state, i.e., the product of the diagonal elements of the matrices shown in Tables II–IV. However, these products are all smaller than 0.04, far smaller than the probabilities of 25–45 % found in these calculations. These results show that the many-body states obtained with two-body random forces are strongly correlated. This correlation in their energies is not, however, associated with quadrupole coherence, which is lost for pure random forces [11]. The subtle connection between correlation and coherence requires further analysis.

The *correlation r* for each value of the mixing parameter *b*, between the states with energies E_J and E_{J+2} in the sample, can be quantitatively calculated [17] as

$$r=\frac{\mathrm{cov}(E_J,E_{J+2})}{\sigma_{E_J}\sigma_{E_{J+2}}}, \tag{4}$$

where

$$\mathrm{cov}(E_J,E_{J+2})=\frac{\sum_i^n (E_{Ji}-E_J)(E_{(J+2)i}-E_{J+2})}{n}. \tag{5}$$

Here, $\mathrm{cov}(E_J,E_{J+2})$ is the covariance of the two distributions, σ is the square root of the variance $\mathrm{cov}(E_J,E_J)$, and n is the size of the space. If $r=1$, the distributions are fully correlated, while if $r\approx 0$ there is no correlation between them. In Table VII the correlation *r* for pairs of energies in the ground-state band of ^{48}Cr are listed.

TABLE VII. Correlations *r* between neighboring states in ^{48}Cr.

$J,J+2$	0.2	0.4	0.6	0.8	1.0
0+,2+	0.966	0.928	0.937	0.949	0.991
2+,4+	0.996	0.991	0.991	0.991	0.986
4+,6+	0.992	0.977	0.974	0.981	0.980
6+,8+	0.991	0.989	0.992	0.993	0.993
8+,10+	0.987	0.989	0.989	0.989	0.987
10+,12+	0.985	0.982	0.982	0.984	0.985
12+,14+	0.992	0.989	0.987	0.986	0.986
14+,16+	0.992	0.992	0.990	0.989	0.988

The presence of strong correlations between the different wave functions obtained with two-body random forces suggests that the many-body states could be well approximated by a small number of configurations that may correspond to definite shapes, as was found for bosonic models. This would imply that the very large number of shell-model many-body states would be limited or constrained by the geometry imposed by the existence of a two-body Hamiltonian, even for the case that its components are randomly selected [18].

VI. THE DTBRE CASE

In Ref. [8] it was shown that a displaced two-body random ensemble (DTBRE) gives rise to coherent rotor patterns. To complement the present study, we analyze in this section the transition from the realistic KB3 interaction to a DTBRE in the ground-state band of ^{48}Cr. The DTBRE corresponds to matrix elements with a normal distribution centered at $c=-1.0$ MeV and width $\sigma=0.6$ MeV, values that were shown in Ref. [8] to be enough to exhibit some collectivity. Figure 10 shows the evolution of the average energies in the ground-state band of ^{48}Cr as a function of the mixing parameter *b*.

At variance from the results shown in Figs. 1, 2, and 4, when the random component of the interaction increases, the absolute energies continuously decrease. As expected, the ro-

TABLE VIII. Probabilities for states belonging to the ground-state band in ^{48}Cr, to occupy their ordered place, for a DTBRE mixing.

$J+$	$b=0.2$	0.4	0.6	0.8	1.0
0	99.58	99.79	97.71	92.08	88.12
2	98.75	99.27	95.00	86.04	80.31
4	98.96	99.38	95.21	86.46	79.90
6	99.27	99.58	96.35	91.46	87.50
8	99.27	99.69	98.02	94.69	91.15
10	99.58	99.90	98.96	96.77	94.38
12	99.69	99.90	98.65	96.77	95.00
14	99.58	99.58	94.79	90.62	87.92
16	99.58	99.69	95.00	90.42	88.33

tor structure survives the transition from realistic to random interactions, with nearly no changes.

In Table VIII we show the probability for states belonging to the ground-state band in ^{48}Cr, to occupy its expected place. Notice that even for $b=1.0$, when the pure displaced random ensemble is employed, the probability for each state to be in its place is larger than 80%, thus exhibiting a high ordering. The percentage of fully ordered bands for each mixing is equally large: 100% for $b=0.2$, 89% for $b=0.6$, and 70% for $b=1.0$. If the centroid of the DTBRE is displaced to more negative values, like $c=-3.0$ MeV, 100% of the bands are ordered [8]. The distribution of $B(E2)$ probabilities exhibits a clear presence of quadrupole coherence for $c=-1$ MeV. They are concentrated in a narrow peak around the collective $B(E2)$ values for $c=-3$ MeV [8].

Realistic interactions in the pf shell, such as KB3*o*BonnC [20], have their matrix elements asymmetrically distributed, with a long tail for negative values [21] and centroid $c=-0.3$ MeV. About 70% of the 195 matrix elements are negative. In these interactions, the quadrupole collectivity is mostly built up by some particular matrix elements with large negative values. To obtain an average energy spectrum that mimics the experimental one in ^{48}Cr, with interaction matrix elements taken randomly from a Gaussian distribution, a larger displacement ($c=-1.0$ MeV) is required.

VII. SUMMARY AND CONCLUSIONS

The average energies of states with different angular momenta preserve their ordering inside the band when the Hamiltonian is changed smoothly from a realistic to a random one. Ground-state energies increase as a function of the mixing parameter. The quadrupole collectivity is lost when the Hamiltonian is dominated by random two-body forces, and the probability that the ground-state band remains ordered diminishes to 25–45 % in the random limit, which is anyway far larger than the product of the probabilities for each state to be in its place, thus exhibiting the strong correlations between the different wave functions. On the other hand, when displaced two-body random ensembles are employed, the average energies decrease as the random component increases, and the rotor pattern remains unchanged.

ACKNOWLEDGMENTS

The exact diagonalizations were performed with the ANTOINE code. This work was supported in part by the Conacyt, México.

[1] N.V. Zamfir, R.F. Casten, and D.S. Brenner, Phys. Rev. Lett. **72**, 3480 (1994).
[2] C.W. Johnson, G.F. Bertsch, and D.J. Dean, Phys. Rev. Lett. **80**, 2749 (1998).
[3] C.W. Johnson, G.F. Bertsch, D.J. Dean, and I. Talmi, Phys. Rev. C **61**, 014311 (1999).
[4] R. Bijker, A. Frank, and S. Pittel, Phys. Rev. C **60**, 021302 (1999).
[5] R. Bijker and A. Frank, Phys. Rev. Lett. **84**, 420 (2000).
[6] R. Bijker and A. Frank, Phys. Rev. C **62**, 014303 (2000).
[7] M. Horoi, B.A. Brown, and V. Zelevinsky, Phys. Rev. Lett. **87**, 062501 (2001).
[8] V. Velázquez and A.P. Zuker, Phys. Rev. Lett. **88**, 072502 (2002).
[9] Y.M. Zhao, A. Arima, and Y. Yoshinaga, Phys. Rev. C **66**, 064322 (2002).
[10] Y.M. Zhao, A. Arima, and Y. Yoshinaga, Phys. Rev. C **66**, 064323 (2002).
[11] A. Cortes, R.U. Haq, and A.P. Zuker, Phys. Lett. **115B**, 1 (1982).
[12] B.H. Wildenthal, Prog. Part. Nucl. Phys. **11**, 5 (1984).
[13] T.T.S. Kuo and G.E. Brown, Nucl. Phys. **A114**, 235 (1968); A. Poves and A.P. Zuker, Phys. Rep. **70**, 235 (1981).
[14] M. Dufour and A.P. Zuker, Phys. Rev. C **54**, 1641 (1996).
[15] E. Caurier, computer code ANTOINE (CRN, Strasbourg, 1989).
[16] Y.M. Zhao, A. Arima, and Y. Yoshinaga, Phys. Rev. C **66**, 034302 (2002).
[17] *Estadística Modelos y Métodos*, edited by D. Peña Sánchez (Alianza Universidad, Textos, 1986).
[18] P. Chau, A. Frank, N. Smirnova, and P. Van Isacher, Phys. Rev. C **66**, 061302(R) (2002).
[19] A.P. Zuker, J. Retamosa, A. Poves, and E. Caurier, Phys. Rev. C **52**, R1741 (1995).
[20] R. Machleidt, Adv. Nucl. Phys. **19**, 189 (1989).
[21] V. Velázquez and A.P. Zuker, Rev. Mex. Fís. **48**, Suppl. 2, 83 (2002).